Pseudopotentials for two-dimensional ultracold scattering in the presence of synthetic spin-orbit coupling

Christiaan R. Hougaard, Brendan C. Mulkerin, Xia-Ji Liu, Hui Hu, and Jia Wang*
Centre for Quantum and Optical Science, Swinburne University of Technology, Melbourne 3122, Australia

(Received 10 October 2019; published 27 December 2019)

We derive a pseudopotential in two dimensions (2D) with a 2D Rashba spin-orbit coupling (SOC), following in the same spirit of the frame transformation by Guan and Blume [Q. Guan and D. Blume, Phys. Rev. A **95**, 020702(R) (2017)]. The frame transformation correctly describes the nontrivial phase accumulation and partial-wave couplings due to the presence of SOC, which modifies the original Fermi pseudopotential in free space, even when the length scale of the SOC is significantly larger than the two-body potential range. As an application, we apply our pseudopotential within the Lippmann-Schwinger equation to obtain an analytical scattering matrix. To demonstrate the validity of our approach, we compare our results with a numerical scattering calculation of the finite-range potential that shows excellent agreement over a wide range of scattering energies and SOC strengths. Our pseudopotential is applicable in the cases of a strong energy-dependent s-wave scattering length and/or non-negligible p-wave interaction, where the original free-space pseudopotential fails. It sets an ideal starting point to explore many-body physics in the presence of synthetic SOC in cold atoms.

DOI: 10.1103/PhysRevA.100.062713

I. INTRODUCTION

Modeling fundamental two-body interactions is one of the most critical steps in investigating the complex quantum physics of many-body systems. In particular, for systems with short-range interactions at low energies, such as ultracold quantum gases, the two-body interaction can be replaced by a zero-range pseudopotential giving the same wave function outside the original potential. One only needs energy-dependent scattering lengths obtained via a partial expansion of the two-body scattering to characterize the strength of such a pseudopotential. For example, in many cases, the s-wave scattering dominates at near-zero temperature, and the Fermi pseudopotential [1,2] gives a highly accurate description of the behavior of degenerate quantum gases. For higher temperatures beyond the Wigner-threshold regime, generalizing the Fermi pseudopotential with an energy-dependent s-wave scattering length gives a quantitative description [3], when the contribution from the higher partial wave is negligible. However, further generalization is needed near resonances of higher partial waves, when the s-wave scattering length vanishes, or when spin-orbit effects couple higher partial waves. These regimes become particularly interesting in the field of quantum gases where interactions can be engineered at will via Feshbach resonances [4]. Even during the initial development of the pseudopotential in the 1950s, Yang and Huang made an early attempt to tackle the generalization to higher partial waves [2]. However, they made an algebraic mistake in their original work, leading to an incorrect prefactor that was discovered and later corrected [5–7]. With the corrected prefactor, the mean-field energy shift of interacting fermions in a trap accurately matches experimental measurements [8].

Extensions of pseudopotentials to lower dimensions for arbitrary partial waves [9] have been of recent interest due to exciting developments in the field of ultracold quantum gases: the creation of low-dimensional systems, which has allowed for the study of various quantum phases and phenomena [10–17]. Another significant development in ultracold quantum gases has been the realization of synthetic gauge fields [18–21], which provide an essential ingredient, namely, spin-orbit coupling (SOC), for the study of nontrivial topological phenomena [22,23].

In previous theoretical studies, the original free-space pseudopotential (obtained from two-body scattering without SOC) is directly applied to the SOC system [19,20]. The justification is based on the argument that the characteristic wavelength of the synthetic SOC is much larger than the inverse of the interaction range. Therefore, SOC is assumed to have no impact on the the wave function at short interparticle distances, and the original pseudopotential remains valid from a perturbation point of view. However, in a foresighted study, Cui [24] pointed out that the presence of SOC at short distances intrinsically mixes different partial waves via the couplings of spin, which leads to a nontrivial influence on the short-range wave function and pseudopotentials. Since this seminal work, several studies have carefully calculated two-body scattering with the presence of three-dimensional (3D) [25–31] or 2D [27,32] SOC. One particularly enlightening study carried out by Guan and Blume [33] revealed that a frame transformation approach (that we will detail later) can correctly calculate the scattering phase accumulated at short distances modified by SOC. However, their approach is difficult to extend to many-body studies and a proper zero-range or δ-shell pseudopotential that includes the

*jiawang@swin.edu.au

nonperturbative effects of SOC at short range and correctly reproduces scattering observables is still missing.

In this paper, we derive an analytical form of the pseudopotential in 2D with the presence of 2D Rashba SOC, following in the same spirit of the frame transformation of Ref. [33]. To test the validity of the pseudopotential, we use the Lippmann-Schwinger equation to obtain the analytical scattering matrix and compare it with a numerical scattering calculation with a finite-range potential.

II. 2D PSEUDOPOTENTIAL WITHOUT SOC

We first give a brief review of the 2D pseudopotential in free space without the presence of SOC. We consider two identical particles ($n = 1, 2$) of mass m confined in a 2D x-y plane with position vectors $\mathbf{r}_n$. Separating out the center-of-mass (COM) motion, the Hamiltonian of the relative motion is given by $H^{\rm fs} = \mathbf{p}^2/2\mu_{2b} + U(\rho)$, where $\mu_{2b} = m/2$ is the two-body reduced mass, $\mathbf{r} = \{\rho, \phi\}$ is the relative position in polar coordinates, and $\mathbf{p} = -i\hbar\{\partial_\rho, \rho^{-1}\partial_\phi\}$ is the relative momentum in 2D. We also assume the potential $U(\rho)$ is isotropic and short range, i.e., vanishes beyond a small radius ρ_0. The isotropic symmetry allows the wave function to be expanded as $\Psi^{\rm fs}(\mathbf{r}) = \sum_{m_\ell} R^{\rm fs}_{m_\ell}(\rho)\Phi_{m_\ell}(\phi)$, where $\Phi_{m_\ell}(\phi) = e^{im_\ell\phi}/\sqrt{2\pi}$ and $R^{\rm fs}_{m_\ell}(\rho)$ satisfies the radial Schrödinger equation,

$$\left[-\frac{\hbar^2}{2\mu_{2b}}\left(\frac{\partial^2}{\partial\rho^2} + \frac{1}{\rho}\frac{\partial}{\partial\rho} - \frac{m_\ell^2}{\rho^2}\right) + U(\rho) - E\right]R^{\rm fs}_{m_\ell}(\rho) = 0, \tag{1}$$

which has an asymptotic form $R^{\rm fs}_{m_\ell}(\rho) \propto J_{m_\ell}(k\rho) - \tan[\delta_{m_\ell}(k)]\, N_{m_\ell}(k\rho)$ for $\rho > \rho_0$. Here, $E = \hbar^2k^2/2\mu_{2b}$ and $J_{m_\ell}(k\rho)$ and $N_{m_\ell}(k\rho)$ are the Bessel functions of the first and second kind, respectively. $\delta_{m_\ell}(k)$ are the energy-dependent phase shifts, satisfying the threshold law $\tan[\delta_0(k)] \propto 1/\log k$ and $\tan[\delta_{m_\ell}(k)] \propto 1/k^{2|m_\ell|}$ for $|m_\ell| \geqslant 1$. Reference [9] shows that replacing $U(\rho)$ by a pseudopotential $V^{\rm fs}_{m_\ell}(\rho)$ can give the same asymptotic wave function, and hence reproduce the low-energy observables of the original finite-range potential. The explicit form of $V^{\rm fs}_{m_\ell}(\rho)$ in free space is given by

$$V^{\rm fs}_{m_\ell}(\rho, k) = -\frac{\hbar^2}{\mu_{2b}}\frac{\tan\left[\delta_{m_\ell}(k)\right]}{c_{m_\ell}k^{2m_\ell}\rho^{m_\ell}}\left[\frac{\delta(\rho - s)}{2\pi\rho}\hat{O}_{m_\ell}(\rho, k)\right]_{s\to 0^+}, \tag{2}$$

where $c_{m_\ell} = (2m_\ell)!/[\Gamma(m_\ell + 1)]^2 2^{2m_\ell}$ and $\Gamma(\cdot)$ is the gamma function. The form of delta shell $\delta(\rho - s)$ of radius s approaches a contact potential $\delta(\rho)$ in the limit $s \to 0$, and allows us to deal with the divergence of the regularized operator rigorously. The regularized operator reads

$$\hat{O}_{m_\ell} = \begin{cases} \frac{2}{1-\tan[\delta_0(k)]f_0(k,\rho)}\frac{\partial}{\partial\rho}\rho, & m_\ell = 0 \\ \frac{2}{1-\tan[\delta_{m_\ell}(k)]f_{m_\ell}(k,\rho)}\frac{\partial^{2m_\ell}}{\partial\rho^{2m_\ell}}\rho^{m_\ell}, & m_\ell > 0, \end{cases} \tag{3}$$

where

$$f_{m_\ell}(k, \rho) = \begin{cases} \frac{2}{\pi}\left[1 + \gamma + \log\left(\frac{1}{2}k\rho\right)\right], & m_\ell = 0 \\ \frac{2}{\pi}\left[\sum_{n=0}^{2m_\ell-1}\frac{1}{2m_\ell - n} - \bar{\psi} + \log\left(\frac{1}{2}k\rho\right)\right], & m_\ell > 0. \end{cases} \tag{4}$$

Here, $2\bar{\psi}(m_\ell) = \psi(1) + \psi(m_\ell + 1)$, where ψ denotes the digamma function. For $m_\ell < 0$, the pseudopotential in Eq. (2) takes the same form, but with m_ℓ replaced by $|m_\ell|$. In contrast to the 3D pseudopotential, the $\tan[\delta_{m_\ell}(k)]$ dependence in the denominator of the regularized operators is unique in 2D and originates from the fact that $\frac{\partial}{\partial\rho}\rho N_0(k\rho)$ and $\frac{\partial^{2m_\ell}}{\partial\rho^{2m_\ell}}\rho^{m_\ell}N_{m_\ell}(k\rho)$ does not vanish at $\rho \to 0$. This constitutes a major difficulty in deriving a pseudopotential with SOC, as we shall discuss below.

III. 2D PSEUDOPOTENTIAL WITH SOC

We consider a 2D Rashba SOC, under which each particle feels a potential, $H^{(n)}_{\rm SO} = k_{\rm SO}\mathbf{p}_n \cdot \mathbf{s}_n/m$, with $\mathbf{p}_n$ and $\mathbf{s}_n$ being the 2D momentum and spin operator of particle n, respectively. Following the method of Refs. [28–31,33], we focus on the scattering in the COM frame, where the relative Hamiltonian can be written as $H_{\rm rel} = H^{\rm fs} + V^{\rm SO}$, where $V^{\rm SO} = k_{\rm SO}\mathbf{\Sigma}\cdot\mathbf{p}/2\mu_{2b}$ describes the SOC effect, and $\mathbf{\Sigma} = \mathbf{s_1} - \mathbf{s_2}$ is the relative spin operator. Here, $k_{\rm SO}$ defines the strength of SOC coupling and gives an energy scale $E_{\rm SO} = \hbar^2k^2_{\rm SO}/2m$.

A formal way to solve the corresponding relative Schrödinger equation is to write it as a multichannel problem by expanding the τth independent solution as

$$\Psi^{\rm SO}_\tau(\mathbf{r}) = \sum_\nu R^{\rm SO}_{\nu\tau}(\rho)A_\nu(\Omega), \tag{5}$$

where the channel functions $A_\nu(\Omega) \equiv \langle\Omega|\nu\rangle$ are functions of Ω that include all degrees of freedom except for ρ. Defining the total spin basis $|\chi\rangle \equiv |(s_1, s_2), S, m_S\rangle$ as usual, where $m_S = m_1 + m_2$ is the quantum numbers of the projection of the operator $\mathbf{S} = \mathbf{s}_1 + \mathbf{s}_2$ to the quantization z axis, we choose the channel functions $A_\nu(\Omega) = i^{m_\ell}\Phi_{m_\ell}(\phi)|\chi\rangle$, with $m_\ell + m_S = m_j$ and $S + m_\ell + s_1 + s_2$ being even or odd for bosons or fermions, respectively. Due to the azimuthal symmetry, total angular momentum (along the z axis) m_j is a good quantum number; therefore we use the subindex ν to collectively represent the quantum numbers $\{m_\ell, S, m_S; m_j\}$. Here we omit the quantum numbers s_1 and s_2 in the channel index notation since they are the same for all channels. At $\rho > \rho_0$, wave functions can be expressed as a linear combination of the noninteracting (with the presence of SOC) regular and irregular solutions $\underline{R}^{\rm SO} = \underline{F} - \underline{G}\underline{\mathcal{K}}$, where $\underline{R}^{\rm SO}$ is the matrix form of the radial solution $R^{\rm SO}_{\nu\tau}(\rho)$ [34]. The matrix elements of the regular solutions $\underline{F}$ can be written as $F_{\nu\tau}(\rho) = N_\tau C_{\nu\tau}\sqrt{k_\tau}J_{m_\ell}(k_\tau\rho)$, where $C_{\nu\tau}$, k_τ, and N_τ can be obtained by diagonalizing the noninteracting Hamiltonian using the same procedure as Ref. [29] and will be provided later for a specific example. The corresponding irregular solutions can be obtained as $G_{\nu\tau}(\rho) = N_\tau C_{\nu\tau}\sqrt{k_\tau}N_{m_\ell}(k_\tau\rho)$. The scattering K matrix $\underline{\mathcal{K}}$ determines the scattering observables and is related to the more familiar S matrix by $\underline{\mathcal{S}} = (\underline{I} + i\underline{\mathcal{K}})(\underline{I} - i\underline{\mathcal{K}})^{-1}$. Our goal is to replace the potential $U(\rho)$ by a pseudopotential $\underline{V}^{(m_j)}(\rho)$ that acts only at $\rho = 0$, and gives the same asymptotic wave function and hence the same K matrix. Here the underline indicates that $\underline{V}^{(m_j)}(\rho)$ is a matrix and not necessarily diagonal due to the presence of SOC.

To derive the pseudopotential, we apply a frame transformation approach in the same spirit of Ref. [33].

Defining a unitary transformation $\mathcal{U}_1 = \exp(-ik_{\rm SO}\mathbf{\Sigma}\cdot\mathbf{r}/2\hbar)$, the "rotated" Hamiltonian $H^{\rm temp} \equiv \mathcal{U}_1^{-1}H_{\rm rel}\mathcal{U}_1 = H^{\rm fs} + \epsilon^{\rm temp} + O(\rho)$ is introduced as an intermediate step. Here, we neglect terms of order ρ and higher, denoted by $O(\rho)$, since the pseudopotential will only act at $\rho = 0$. The constant term $\epsilon^{\rm temp}$ is given by $\epsilon^{\rm temp} = -E_{\rm SO}(\Sigma_x^2 + \Sigma_y^2 + S_zL_z)/2\hbar^2$, where Σ_x (Σ_y) is the x (y) component of $\mathbf{\Sigma}$, S_z is the z component of total spin operator $\mathbf{S}$, and $L_z = -i\hbar\partial_\phi$ is the 2D angular momentum operator. For two spin-1/2 particles, this operator expanded by the channel functions $A_\nu(\Omega)$ gives a diagonal matrix $\underline{\epsilon}^{\rm temp}$. For higher spins, $\underline{\epsilon}^{\rm temp}$ is, in general, not diagonal, where the nonzero matrix elements are the ones which couple channels with the same m_S and hence the same m_ℓ. Therefore, one can introduce another ρ-independent unitary transformation $\mathcal{U}_2$ that is block diagonal in m_ℓ subspace and satisfies $\underline{\epsilon} = \mathcal{U}_2^{-1}\underline{\epsilon}^{\rm temp}\mathcal{U}_2$, which is diagonal. Automatically, $\mathcal{U}_2^{-1}H^{\rm fs}\mathcal{U}_2 = H^{\rm fs}$ is also diagonal. Therefore, we find a unitary transformation $\mathcal{U} = \mathcal{U}_2\mathcal{U}_1$ that leads to a set of uncoupled radial Schrödinger equations that are at least valid near the origin $\rho = 0$, which is given by

$$\left[-\frac{\hbar^2}{2\mu_{2b}}\left(\frac{\partial^2}{\partial\rho^2} + \frac{1}{\rho}\frac{\partial}{\partial\rho} - \frac{m_\ell^2}{\rho^2}\right) + U(\rho) - E_\nu\right]\tilde{R}^{\rm SO}_{\nu\nu}(\rho) = 0, \tag{6}$$

where $E_\nu \equiv E + \epsilon_\nu$, and ϵ_ν are the diagonal matrix elements of SOC-induced energy shift $\underline{\epsilon}$. Comparing with the free-space Schrödinger equation in Eq. (1), a pseudopotential $\underline{\tilde{V}}^{(m_j)}(\rho, k)$ with diagonal matrix elements $\tilde{V}^{(m_j)}_{\nu\nu}(\rho, k) = V^{\rm fs}_{m_\ell}(\rho, k_\nu)$, where $k_\nu = \sqrt{2\mu_{2b}E_\nu}$, can reproduce the wave function $\tilde{R}^{\rm SO}_{\nu\nu}(\rho)$ in the rotated frame. The pseudopotential in the original frame can therefore be obtained by an inverse rotation,

$$\underline{V}^{(m_j)}(\rho, k) = \mathcal{U}\underline{\tilde{V}}^{(m_j)}(\rho, k)\mathcal{U}^{-1}. \tag{7}$$

Once we have obtained $\underline{V}^{(m_j)}(\rho, k)$ for all m_j (or up to a cutoff in practice), the total pseudopotential can be expressed in a general form as

$$V(\rho, k)\Psi^{\rm SO}(\mathbf{r}) = \sum_{m_j}\sum_{\nu\nu'}A_\nu(\Omega)\int d\rho'\delta(\rho-\rho')\underline{V}^{(m_j)}_{\nu\nu'}(\rho', k) \times \int d\Omega' A^*_{\nu'}(\Omega')\Psi^{\rm SO}(\mathbf{r}'). \tag{8}$$

IV. AN ILLUSTRATIVE EXAMPLE

Here, we consider two spin-1/2 fermions in the $m_j = 0$ subspace, and omit the notation of m_j hereafter unless otherwise specified. The basis is denoted by $\nu \equiv \{m_\ell, S, m_S\} = \{-1, 1, 1\}, \{0, 0, 0\}, \{1, 1, -1\}$. In this order of the basis, the rotational matrix can be written out explicitly,

$$\underline{\mathcal{U}} = \begin{bmatrix} \cos^2\left(\frac{\lambda\rho}{2}\right) & -\frac{\sin(\lambda\rho)}{\sqrt{2}} & -\sin^2\left(\frac{\lambda\rho}{2}\right) \\ \frac{\sin(\lambda\rho)}{\sqrt{2}} & \cos(\lambda\rho) & \frac{\sin(\lambda\rho}{\sqrt{2}} \\ -\sin^2\left(\frac{\lambda\rho}{2}\right) & -\frac{\sin(\lambda\rho)}{\sqrt{2}} & \cos^2\left(\frac{\lambda\rho}{2}\right) \end{bmatrix}, \tag{9}$$

where $\lambda = k_{\rm SO}/2$ is introduced for convenience. After rotation, the SOC-induced energy shift is given by $\underline{\epsilon} = {\rm diag}[0, \hbar^2\lambda^2/\mu_{2b}, 0]$, where diag[·] represents a diagonal matrix. The energy shift determines the pseudopotential in the rotated frame as $\underline{\tilde{V}}(\rho, k) = {\rm diag}[V_1^{\rm fs}(\rho, k_p), V_0^{\rm fs}(\rho, k_s), V_1^{\rm fs}(\rho, k_p)]$, where $k_s = \sqrt{k^2 + 2\lambda^2}$ and $k_p = k$. We then apply Eq. (7) to obtain the pseudopotential in the original frame as a summation of s- and p-wave contributions with notations $\delta_s \equiv \delta_0$ and $\delta_p \equiv \delta_1$:

$$\underline{V} = -\frac{\hbar^2}{\mu_{2b}}\left\{\frac{\delta(\rho-s)}{2\pi\rho}\left[\tan\delta_s(k_s)\underline{O}_s + \frac{\tan\delta_p(k_p)}{k_p^2}\underline{O}_p\right]\right\}_{s\to 0}, \tag{10}$$

where

$$\underline{O}_s = \begin{bmatrix} 0 & 0 & 0 \\ -\frac{\lambda}{\sqrt{2}}\hat{O}_0\rho & \frac{1}{\rho}\hat{O}_0 & -\frac{\lambda}{\sqrt{2}}\hat{O}_0\rho \\ 0 & 0 & 0 \end{bmatrix} \tag{11}$$

and

$$\underline{O}_p = \begin{bmatrix} \frac{1}{\rho}\hat{O}_1\left(1-\frac{\lambda^2\rho^2}{4}\right) & \frac{\lambda}{\rho\sqrt{2}}\hat{O}_1\rho & -\frac{1}{\rho}\hat{O}_1\frac{\lambda^2\rho^2}{4} \\ \frac{\lambda}{\sqrt{2}}\hat{O}_1\left(1-\frac{\lambda^2\rho^2}{2}\right) & \lambda^2\hat{O}_1\rho & \frac{\lambda}{\sqrt{2}}\hat{O}_1\left(1-\frac{\lambda^2\rho^2}{2}\right) \\ -\frac{1}{\rho}\hat{O}_1\frac{\lambda^2\rho^2}{4} & \frac{\lambda}{\rho\sqrt{2}}\hat{O}_1\rho & \frac{1}{\rho}\hat{O}_1\left(1-\frac{\lambda^2\rho^2}{4}\right) \end{bmatrix}. \tag{12}$$

Terms higher than the order of ρ can be ignored with the consideration that the pseudopotential only contributes to the K matrix with terms proportional to $F^*_{\nu'\tau'}(s)V_{\nu'\nu}(s, k)F_{\nu\tau}(s)_{s\to 0}$ and $F^*_{\nu'\tau'}(s)V_{\nu'\nu}(s, k)G_{\nu\tau}(s)_{s\to 0}$ [see Eqs. (15) below]. Comparing with the free-space pseudopotential diag$[V_1^{\rm fs}(k, \rho), V_0^{\rm fs}(k, \rho), V_1^{\rm fs}(k, \rho)]$, there are two important differences. One is that the SOC-induced energy shift leads to a different s-wave phase shift $\delta_s(k_s)$. The other is the nondiagonal terms from the rotational transformation, which describes the intrinsic partial-wave mixing at short distances induced by the SOC. As we will see, both of these differences play a significant role in correctly producing scattering observable.

V. LIPPMANN-SCHWINGER EQUATION

To verify the validity of the above pseudopotential, we apply the Lippmann-Schwinger equation to calculate the K matrix. The Lippmann-Schwinger equation is the integral form of the Schrödinger equation $\Psi_\tau(\mathbf{r}) = \Psi_0(\mathbf{r}) + \int G(\mathbf{r}, \mathbf{r}')U(\mathbf{r}')\Psi_\tau(\mathbf{r}')d\mathbf{r}'$ or, equivalently, in matrix form,

$$\underline{R}^{\rm SO}(\rho) = \underline{F}(\rho) + \int \underline{\mathcal{G}}(\rho, \rho')\underline{U}(\rho')\underline{R}^{\rm SO}(\rho')\rho' d\rho'. \tag{13}$$

Here, $\underline{\mathcal{G}}(\rho, \rho')$ is the matrix representation of the Green's function $\mathcal{G}(\mathbf{r}, \mathbf{r}') = \sum_{\nu\nu'}A_\nu(\Omega)\underline{\mathcal{G}}_{\nu\nu'}(\rho, \rho')A^*_{\nu'}(\Omega')$, which is given by

$$\underline{\mathcal{G}}(\rho, \rho') = \pi\begin{cases}\underline{F}(\rho)\underline{G}^\dagger(\rho'), & \rho < \rho' \\ \underline{G}(\rho)\underline{F}^\dagger(\rho'), & \rho > \rho'.\end{cases} \tag{14}$$

Replacing the potential $\underline{U}(\rho')$ by a pseudopotential $\underline{V}(\rho') \propto \delta(\rho')$ from Eq. (10), the K matrix can then be obtained by

$\underline{\mathcal{K}} = (I + \underline{\mathcal{B}})^{-1}\underline{\mathcal{A}}$, where

$$\underline{\mathcal{A}} = -\pi \int \rho' d\rho' \underline{F}^{\dagger}(\rho')\underline{V}(\rho')\underline{F}(\rho'),$$
$$\underline{\mathcal{B}} = -\pi \int \rho' d\rho' \underline{F}^{\dagger}(\rho')\underline{V}(\rho')\underline{G}(\rho'). \tag{15}$$

Notice that a special property of 2D is that the matrix $\underline{\mathcal{B}}$ does not vanish since $\frac{\partial}{\partial\rho}\rho N_0(k_\tau\rho)$ and $\frac{\partial^{2m_\ell}}{\partial\rho^{2m_\ell}}\rho^{m_\ell}N_{m_\ell}(k\rho)$ does not vanish at $\rho \to 0$ [35]. As a direct consequence of this property, the K matrix, in general, cannot be written as a summation of s- and p-wave contributions, in contrast to the 3D case as shown in Eq. (11) of Ref. [33].

For our example of two spin-1/2 fermions in the $m_j = 0$ subspace, the regular $\underline{F}$ and irregular solutions $\underline{G}$ can be determined by the coefficients $C_{\nu\tau}$ in matrix form,

$$\underline{C} = \begin{bmatrix} -1/2 & -1/2 & 1/\sqrt{2} \\ -1/\sqrt{2} & 1/\sqrt{2} & 0 \\ 1/2 & 1/2 & 1/\sqrt{2} \end{bmatrix}, \tag{16}$$

where the column index τ corresponds to canonical momentum $\{k_\tau\} \equiv \{k_1, k_2, k_3\} = \{k_b + \lambda, k_b - \lambda, k\}$ and normalization $\{\hbar^2 N_\tau^2/\mu_{2b}\} = \{1/k_b, 1/k_b, 1/k\}$, where $k_b = \sqrt{\lambda^2 + k^2}$. One can identify $\tau = \{1, 2, 3\}$ corresponding to three different configurations $|-,-\rangle$, $|+,+\rangle$, and $|-,+\rangle$, where $-$ $(+)$ indicates the helicity, i.e., whether the spin is antiparallel (parallel) to the direction of current [28].

Inserting $\underline{F}$ and $\underline{G}$ into Eq. (15) gives $\underline{\mathcal{A}}$ and $\underline{\mathcal{B}}$, which determines $\underline{\mathcal{K}}$. We find that the K matrix is block diagonal and can be expressed as

$$\underline{\mathcal{K}} = \begin{bmatrix} \underline{\mathcal{K}}^{(+)} & 0 \\ 0 & \underline{\mathcal{K}}^{(-)} \end{bmatrix}, \tag{17}$$

where $\underline{\mathcal{K}}^{(-)} = \tan[\delta_p(k_p)]$, and $\underline{\mathcal{K}}^{(+)}$ is a 2×2 matrix. The block-diagonal structure can be understood by studying the $\mathcal{PT}$ symmetry of $\sum_\nu F_{\nu\tau}(\rho)A_\nu(\Omega)$ in the $m_j = 0$ subspace, where $\mathcal{P}$ is defined as $\phi \to \phi + \pi$ and $\mathcal{T}$ is defined as $|s_n, m_n\rangle \to |s_n, -m_n\rangle$ for both $n = 1, 2$. Defining $\mathcal{PT}[\sum F_{\nu\tau}(\rho)A_\nu(\Omega)] = \Pi_\tau[\sum F_{\nu\tau}(\rho)A_\nu(\Omega)]$, one finds that $\Pi_\tau = +1/-1$ for $\tau = \{1, 2\}/\{3\}$, leading to the block-diagonal structure [36]. The elements of $\underline{\mathcal{K}}^{(+)}$ are analytical but quite cumbersome, and hence we only give the full expression in the Supplemental Material [35] and illustrate them in Figs. 1 and 2 as two numerical examples near s- and p-wave resonances, respectively. In these two examples, the energy-dependent phase shifts $\delta_s(k)$ and $\delta_p(k)$ are obtained from a free-space scattering calculation with Lennard-Jones potential $U(\rho) = -\frac{C_6}{\rho^6}(1 - \frac{r_0^6}{\rho^6})$, where C_6 defines a length scale $r_{\rm vdW} = (2\mu_{2b}C_6/\hbar^2)^{1/4}/2$ and r_0 controls the short-range physics, which is used to tune zero-energy scattering phase shifts. The analytical results show good agreement with the full numerical scattering calculation [31], which is carried out by solving time-independent coupled Schrödinger equations with Lennard-Jones potential as shown in the Supplemental Material [35].

Near an s-wave resonance, p-wave scattering is negligible and the scattering matrix can be simplified as

$$\underline{\mathcal{K}}^{(s)} = T_0 \begin{bmatrix} k_1 & -k \\ -k & k_2 \end{bmatrix}, \tag{18}$$

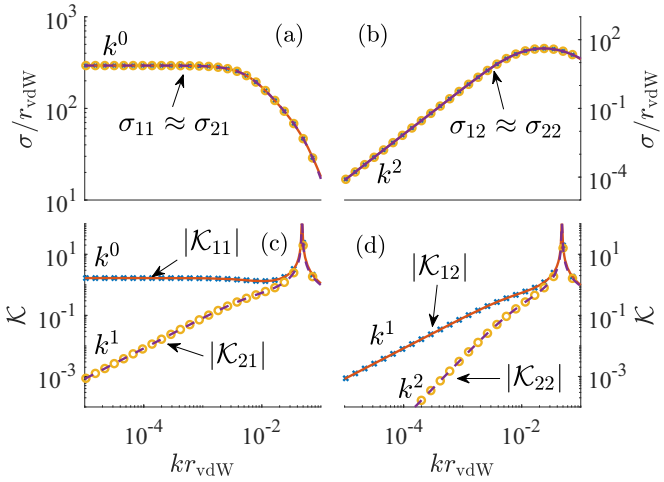

FIG. 1. Results near s-wave resonances with $\lambda r_{\rm vdW} = 0.01$. The free-space scattering phase shifts are obtained from a Lennard-Jones model potential with parameter $r_0 = 0.58 r_{\rm vdW}$ that leads to $a_s(0) \approx 21.777 r_{\rm vdW}$. (a),(b) Partial cross sections. (c),(d) K-matrix elements. The curves represent analytical results and the symbols are obtained by numerical scattering calculations.

where $T_0 = \tan[\delta_s(k_s)]/2k_b\alpha_s$ and $\alpha_s = 1 + \frac{2}{\pi}\tan[\delta_s(k_s)](\log\frac{k}{k_s} + \frac{\lambda}{k_b}\tanh^{-1}\frac{\lambda}{k_b})$. The S matrix can be obtained via $\underline{\mathcal{S}}^{(s)} = (I + i\underline{\mathcal{K}}^{(s)})(I - i\underline{\mathcal{K}}^{(s)})^{-1}$ and determines the scattering cross section $\sigma_{\tau\tau'}^{(s)} = 2|\underline{\mathcal{S}}_{\tau\tau'}^{(s)} - \delta_{\tau\tau'}|^2/k_\tau$, which are given by $\sigma_{11}^{(s)} = \sigma_{21}^{(s)} = k_1 8T_0^2/(1 + 4T_0^2k_b^2)$ and $\sigma_{12}^{(s)} = \sigma_{22}^{(s)} = k_2 8T_0^2/(1 + 4T_0^2k_b^2)$. As a result, $\sigma_{21}^{(s)}/\sigma_{12}^{(s)} = k_1/k_2 > 1$ indicates that particles are preferentially scattered into the lower-energy helicity "$-$" state. The validity of Eq. (18) near an s-wave resonance can be seen in Fig. 1. In the zero-energy limit, we find $\lambda\sigma_{11}^{(s)} \to 4/(1 + \{\gamma + \frac{2}{\pi}\log[\lambda a_s(\sqrt{2}\lambda)]\}^2)$, where $a_s(k)$ is the generalized energy-dependent s-wave

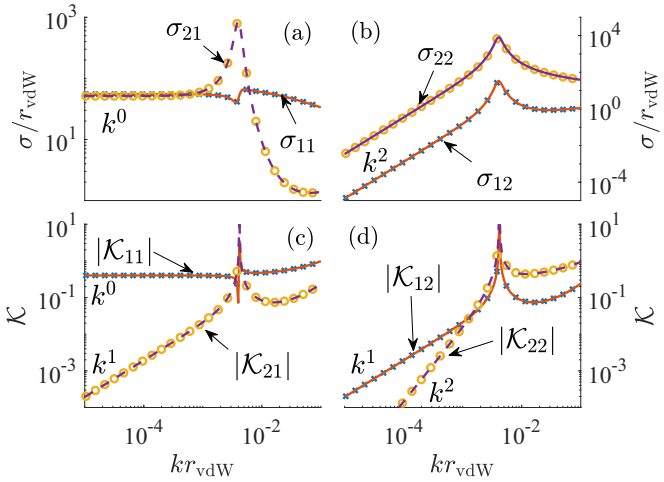

FIG. 2. Results near p-wave resonances with $\lambda r_{\rm vdW} = 0.01$. The free-space scattering phase shifts are obtained from a Lennard-Jones model potential with parameter $r_0 = 0.552981 r_{\rm vdW}$ that leads to $A_p \approx -8.577 \times 10^5 r_{\rm vdW}^2$. (a),(b) Partial cross sections. (c),(d) K-matrix elements. The curves represent analytical results and the symbols are obtained by numerical scattering calculations.

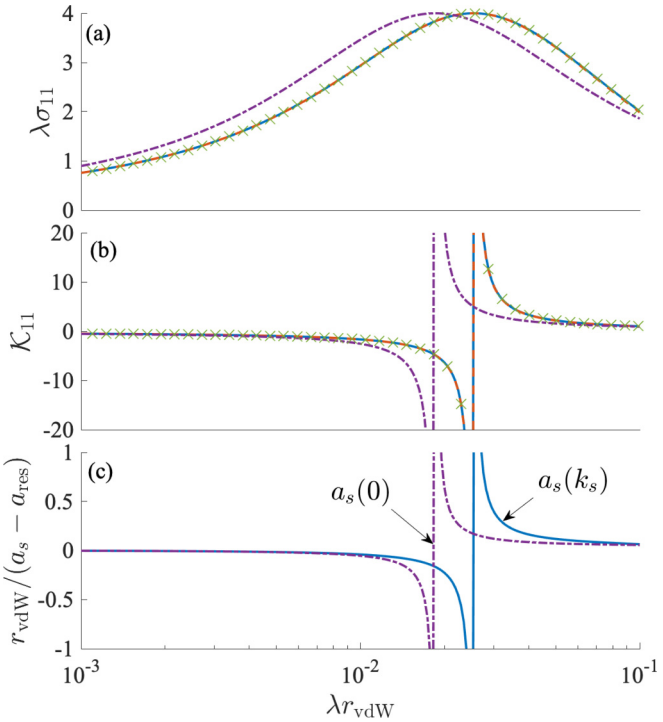

FIG. 3. Scattering results at zero scattering energy for the same Lennard-Jones potential of Fig. 1. (a) Scaled partial cross section $\lambda\sigma_{11}$ as a function of λ. (b) K-matrix element $\mathcal{K}_{11}$ as a function of λ. The blue solid curves are the analytical results, and the red dashed curves are determined by the s-wave only approximation in Eq. (18), which are indistinguishable from the solid curves on the scale that is shown. The purple dash-dotted curves are calculated using the free-space pseudopotential directly. The green crosses are results from a numerical calculation using the same Lennard-Jones potential with the presence of SOC. (c) The blue solid curve shows $r_{\rm vdW}/[a_s(k_s) - a_{\rm res}]$ as a function of λ, while the purple dash-dotted curve shows $r_{\rm vdW}/[a_s(0) - a_{\rm res}]$.

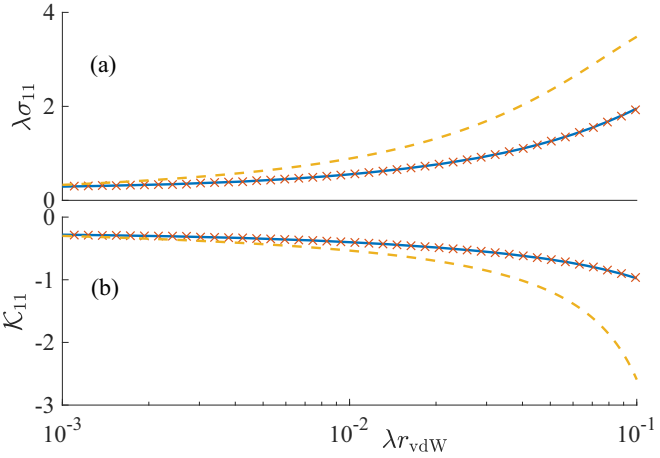

FIG. 4. Scattering results at zero scattering energy for the same Lennard-Jones potential in Fig. 2. (a) Scaled partial cross section $\lambda\sigma_{11}$ as a function of λ. (b) K-matrix element $\mathcal{K}_{11}$ as a function of λ. The blue solid curves are the analytical results, and the yellow dashed curves are determined by the s-wave only approximation in Eq. (18). The red crosses are results from a numerical calculation using the same Lennard-Jones potential with the presence of SOC.

scattering length defined by $\cot[\delta_s(k)] = \frac{2}{\pi}\log[ka_s(k)] + \gamma$, and the rescaled cross section therefore reaches a maximum when $a_s(k_s)$ equals $a_{\rm res} \equiv e^{-\pi\gamma/2}/\lambda$. In comparison, if we replace $U(\rho)$ directly by $\mathrm{diag}[0, V_0^{\rm fs}(k,\rho), 0]$, i.e., the free-space pseudopotential with s-wave scattering only, and apply the Lippmann-Schwinger equation, the resulting K matrix will be the same as Eq. (18), with k_s replaced by k. Consequently, the rescaled cross section reaches a maximum when $a_s(0) = a_{\rm res}$. In Fig. 3(a), we show this comparison, where one can see that the SOC-induced energy shift that leads to $k_s \neq k$ is crucial to characterize the two-body scattering correctly, especially near the maximum of $\lambda\sigma_{11}$.

Near p-wave resonances, the p-wave phase shift can no longer be neglected. Nevertheless, a simplified formula can be obtained in the low-energy limit $k \to 0$, where $\tan[\delta_s(k_s)] \to -A_s \equiv -\tan[\delta_s(\sqrt{2}\lambda)]$ and $\tan[\delta_p(k_p)] \to -A_p k^2$, and the K matrix is given by

$$\lim_{k\to 0} \underline{\mathcal{K}}^{(+)} = \frac{1}{d}\begin{bmatrix} b_{11} & b_{12}k/\lambda \\ b_{21}k/\lambda & b_{22}k^2/\lambda^2 \end{bmatrix}. \tag{19}$$

Here, d and $b_{\tau'\tau}$ are constants, where $d = 1 - 2(\log\sqrt{2})A_s/\pi - 2\lambda^2 A_p/\pi + 4\lambda^2 A_p A_s[(\log\sqrt{2}) - 1]/\pi^2$, $b_{11} = -A_s(1/2 - \lambda^2 A_p/\pi)$, $b_{12} = b_{21} = A_s(1/2 + \lambda^2 A_p/\pi)$, and $b_{22} = -A_s/4 - \lambda^2 A_p - \lambda^2 A_p A_s(3/2 - \log 2)/\pi$. When $|\lambda^2 A_p| \gtrsim 1$, p-wave scattering gives a significant contribution as shown in Fig. 4, where Eq. (18) is no longer valid. However, the threshold laws for cross-section and K-matrix elements are valid for all situations, as shown in Figs. 1 and 2. Interestingly, the elastic scattering rate $\propto k_1\sigma_{11}$, which determines thermalization, remains constant in the zero-energy limit, in contrast to the vanishing $1/(\log k)^2$ rate without the presence of SOC. We also remark here that using the free-space pseudopotential including the p-wave contribution $\mathrm{diag}[V_1^{\rm fs}(k,\rho), V_0^{\rm fs}(k,\rho), V_1^{\rm fs}(k,\rho)]$ will incorrectly give a vanishingly small K matrix due to a $\log(s)|_{s\to 0}$ term in the denominator of all the matrix elements of $\underline{\mathcal{K}}^{(+)}$, reflecting the importance of the nondiagonal terms in the pseudopotential.

VI. SUMMARY

We have derived a pseudopotential in the COM frame with the presence of SOC in 2D using a frame-transformation approach. We found that the s-wave scattering phase shift changes due to an SOC-induced energy shift and the frame transformation introduces nondiagonal terms, which are essential to reproduce the correct two-body scattering observables. We applied the pseudopotential within the Lippmann-Schwinger equation to obtain the analytical scattering matrix and compare it with a numerical scattering calculation with a finite-range potential. Our pseudopotential is valid even near s- or p-wave resonances for $\lambda r_{\rm vdW} \ll 1$, which is usually well satisfied in ultracold quantum gases. Our results indicate that if we consider s-wave scattering only (which usually implies scattering near an s-wave resonance), and the energy dependency of $a_s(k)$ is very weak (which usually implies a very broad resonance) so that $a_s(\sqrt{2}\lambda) \approx a_s(0)$, the free-space pseudopotential gives a good approximation, i.e., within the

regime of previous studies in Refs. [27,32]. On the other hand, if the energy dependency of $a_s(k)$ is strong or the p-wave interaction is non-negligible, our pseudopotential has to be adopted in order to reproduce the correct two-body scattering.

Our approach can easily be applied in 3D and reproduce Eq. (11) of Ref. [33], which we will detail elsewhere. Our results are also useful for investigating universal relations and Tan's contacts for SOC quantum gases in 2D [37] and might eventually be applied in many-body studies. In particular, we expect that the interesting intrinsic partial-wave mixing at short range induced by SOC represented by the off-diagonal matrix elements in our pseudopotential might lead to interesting many-body effects.

[1] E. Fermi, Nuovo Cimento **11**, 157 (1934).
[2] K. Huang and C. N. Yang, Phys. Rev. **105**, 767 (1957).
[3] E. L. Bolda, E. Tiesinga, and P. S. Julienne, Phys. Rev. A **66**, 013403 (2002).
[4] C. Chin, R. Grimm, P. Julienne, and E. Tiesinga, Rev. Mod. Phys. **82**, 1225 (2010).
[5] R. Stock, A. Silberfarb, E. L. Bolda, and I. H. Deutsch, Phys. Rev. Lett. **94**, 023202 (2005).
[6] A. Derevianko, Phys. Rev. A **72**, 044701 (2005).
[7] Z. Idziaszek and T. Calarco, Phys. Rev. Lett. **96**, 013201 (2006).
[8] R. Roth and H. Feldmeier, Phys. Rev. A **64**, 043603 (2001).
[9] K. Kanjilal and D. Blume, Phys. Rev. A **73**, 060701(R) (2006).
[10] I. Bloch, J. Dalibard, and W. Zwerger, Rev. Mod. Phys. **80**, 885 (2008).
[11] B. Paredes, A. Widera, V. Murg, O. Mandel, S. Fölling, I. Cirac, G. V. Shlyapnikov, T. W. Hänsch, and I. Bloch, Nature(London) **429**, 277 (2004).
[12] T. Kinoshita, T. Wenger, and D. S. Weiss, Science **305**, 1125 (2004).
[13] Z. Hadzibabic, P. Krüger, M. Cheneau, B. Battelier, and J. Dalibard, Nature **441**, 1118 (2006).
[14] P. Cladé, C. Ryu, A. Ramanathan, K. Helmerson, and W. D. Phillips, Phys. Rev. Lett. **102**, 170401 (2009).
[15] S. P. Rath, T. Yefsah, K. J. Günter, M. Cheneau, R. Desbuquois, M. Holzmann, W. Krauth, and J. Dalibard, Phys. Rev. A **82**, 013609 (2010).
[16] Y. Nishida, S. Moroz, and D. T. Son, Phys. Rev. Lett. **110**, 235301 (2013).
[17] C. Gao, J. Wang, and Z. Yu, Phys. Rev. A **92**, 020504(R) (2015).
[18] Y.-J. Lin, K. Jiménez-García, and I. B. Spielman, Nature (London) **471**, 83 (2011).
[19] J. Zhang, H. Hu, X.-J. Liu, and H. Pu, Annu. Rev. Cold At. Mol. **2**, 81 (2014).
[20] H. Zhai, Rep. Prog. Phys. **78**, 026001 (2015).
[21] J. Struck, C. Ölschläger, M. Weinberg, P. Hauke, J. Simonet, A. Eckardt, M. Lewenstein, K. Sengstock, and P. Windpassinger, Phys. Rev. Lett. **108**, 225304 (2012).
[22] J. Dalibard, F. Gerbier, G. Juzeliūnas, and P. Öhberg, Rev. Mod. Phys. **83**, 1523 (2011).
[23] N. Goldman, G. Juzeliunas, P. Öhberg, and I. B. Spielman, Rep. Prog. Phys. **77**, 126401 (2014).
[24] X. Cui, Phys. Rev. A **85**, 022705 (2012).
[25] P. Zhang, L. Zhang, and Y. Deng, Phys. Rev. A **86**, 053608 (2012).
[26] Z. Yu, Phys. Rev. A **85**, 042711 (2012).
[27] L. Zhang, Y. Deng, and P. Zhang, Phys. Rev. A **87**, 053626 (2013).
[28] H. Duan, L. You, and B. Gao, Phys. Rev. A **87**, 052708 (2013).
[29] S.-J. Wang and C. H. Greene, Phys. Rev. A **91**, 022706 (2015).
[30] Q. Guan and D. Blume, Phys. Rev. A **94**, 022706 (2016).
[31] J. Wang, C. R. Hougaard, B. C. Mulkerin, and X.-J. Liu, Phys. Rev. A **97**, 042709 (2018).
[32] P. Zhang, L. Zhang, and W. Zhang, Phys. Rev. A **86**, 042707 (2012).
[33] Q. Guan and D. Blume, Phys. Rev. A **95**, 020702(R) (2017).
[34] Throughout this paper, underline implies matrix form.
[35] See Supplemental Material at http://link.aps.org/supplemental/10.1103/PhysRevA.100.062713 for the details of (I) the technical details of the Lippman-Schwinger formalism in 2D, (II) the full analytical expression of the K matrix, and (III) technical details of our numerical method .
[36] For $m_j \neq 0$ subspaces, sign(m_j) and $\mathcal{PT}$ cannot simultaneously be good quantum numbers.
[37] C.-X. Zhang, S.-G. Peng, and K. Jiang, arXiv:1907.11433.